Journal of Molecular Catalysis B: Enzymatic 84 (2012) 15–21

Contents lists available at SciVerse ScienceDirect

Journal of Molecular Catalysis B: Enzymatic

journal homepage: www.elsevier.com/locate/molcatb

Synthesis of a chiral alcohol using a rationally designed *Saccharomyces cerevisiae* reductase and a NADH cofactor regeneration system

Jihye Jung[a], Seongsoon Park[b], Hyung Kwoun Kim[a,*]

[a] *Division of Biotechnology, The Catholic University of Korea, Bucheon 420-743, Republic of Korea*
[b] *Department of Chemistry, Center for NanoBio Applied Technology, Institute of Basic Sciences, Sungshin Women's University, Seoul 136-742, Republic of Korea*

ARTICLE INFO

Article history:
Available online 25 January 2012

Keywords:
Reductase
Protein engineering
Cofactor preference
NADH
Chiral compound

ABSTRACT

Ethyl (*S*)-4-chloro-3-hydroxy butanoate (ECHB) is a building block for the synthesis of hypercholesterolemia drugs that function as 3-hydroxy-3-methylglutaryl coenzyme A reductase inhibitors. Yeast reductase YDL124W has been shown to convert ethyl 4-chloro-3-oxo butanoate (ECOB) into (*S*)-ECHB in an enantioselective manner. In that reduction, YDL124W absolutely prefers NADPH as a cofactor to NADH. NADPH is, however, much more expensive and unstable than NADH. In this study, four amino acid residues that directly interact with the 2′-phosphate group of adenosine ribose of NADPH were identified based on the homology model and docking model of YDL124W with ECOB and NADPH. Among various single mutants altered in these target residues, R264H evidenced noticeably increased reductase activity with NADH. The double mutant, R264H/R27Y, had more profoundly enhanced reductase activity with NADH. Kinetic analysis results demonstrated that these mutants had reduced K_m values toward NADH and increased k_{cat}/K_m values in comparison with the wild-type. Computer modeling showed that no hydrogen bond could be formed between the wild-type and 2′-hydroxyl group of adenosine ribose of the NADH cofactor, whereas three hydrogen bonds and one π–π stacking interaction could be formed between R264H or R264H/R27Y mutants and the NADH cofactor. These two mutants could efficiently produce (*S*)-ECHB using NADH as a cofactor in conjunction with formate dehydrogenase as a coupling enzyme.

1. Introduction

The asymmetric reduction of ketones to optically pure alcohols has become the focus of a great deal of attention, primarily in regard to their possible use as intermediates for the synthesis of chiral building block. Some microbial reductases are capable of reducing the carbonyl groups of various compounds in a chemo-, regio-, and stereo-selective manner [1,2].

Most reductases require NAD(P)H cofactor for the reduction of ketone substrates. Although many reductases efficiently mediate a variety of enantioselective bioconversion, the cofactor is too expensive for the enzymatic bioconversion to be performed economically [1,3]. To alleviate this cost factor, a cofactor recycling system is usually introduced to the reductase bioconversion: namely, the enzyme coupling reaction of glucose dehydrogenase (GDH) [4–6] or formate dehydrogenase (FDH) [7–9].

NADPH cofactor is much more expensive and unstable than NADH. Unfortunately, many reductases, including aldo-keto reductase (AKR) family members, employ NADPH exclusively as their cofactors, rather than NADH [10]. Several research groups have attempted to alter this cofactor preference by rationally altering the protein structure [11–14].

Katzberg et al. engineered yeast reductase Gre2p via site-directed mutagenesis. The N9E mutant evidenced an enhanced cofactor preference (NADH/NADPH) of 0.9, whereas the wild-type had a preference of 0.007 [12]. Zhang et al. noted that mutant S67D/H68D of *Candida parapsilosis* carbonyl reductase had an altered specificity from NADPH to NADH [15]. Additionally, Banta et al. reported that three amino acids in the cofactor-binding pocket of *Corynebacterium* 2,5-diketo-D-gluconic acid reductase were important for determining cofactor preference, and they constructed a mutant enzyme via combinatorial mutagenesis [11,16]. Shimizu et al. reported *Candida magnolia* reductase could synthesize optically pure ethyl (*S*)-4-chloro-3-hydroxybutanoate [17] and developed *Escherichia coli* transformant cells coexpressing the carbonyl reductase and glucose dehydrogenase genes [18].

In the previous study, we reported *Saccharomyces cerevisiae* YDL124W enzyme capable of generating ethyl (*S*) 4-chloro-3-hydroxy butanoate ((*S*)-ECHB), which was a chiral building block for the synthesis of Atorvastatin, a hyperlipidemia drug [19]. A homology model of YDL124W was constructed on the basis of the X-ray crystal structure of human liver Δ4-3-ketosteroid 5β-reductase

* Corresponding author. Tel.: +82 2 2164 4890; fax: +82 2 2164 4865.
E-mail address: hkkim@catholic.ac.kr (H.K. Kim).

1381-1177/$ – see front matter © 2012 Elsevier B.V. All rights reserved.
doi:10.1016/j.molcatb.2012.01.016

(PDB ID 3BUV) [20]. In addition, its docking model with ethyl 4-chloro-3-oxo butanoate (ECOB) substrate and NADPH cofactor was also constructed, and its possible enantioselective reaction mechanism was elucidated [19].

In this research, we attempted to determine the amino acid residues that interact with the 2′-phosphate group of adenosine ribose of NADPH based on the docking structure. We developed mutant reductases capable of producing (*S*)-ECHB with the NADH cofactor. Their kinetic parameters were determined and computer modeling was conducted. Furthermore, two mutants were used to generate (*S*)-ECHB by using NADH and formate dehydrogenase as a cofactor and a coupling enzyme, respectively.

2. Experimentals

2.1. Chemicals

Ethyl-4-chloro-3-oxo butanoate (ECOB), formate dehydrogenase (FDH, *Candida boidinii*), NAD(P)H, and NAD(P)$^+$ were purchased from Sigma–Aldrich Co. (St. Louis, MO). (*R*)- and (*S*)-ethyl-4-chloro-3-hydroxy butanoate ((*R*)- and (*S*)-ECHB) were received from Cronbio Com (Korea). All other chemicals were of analytical grade.

2.2. Reductase and formate dehydrogenase activity assay

Reductase activity was evaluated at 30 °C by measuring the reduction in absorbance at 340 nm for 5–10 min using a spectrophotometer. The reaction mixture (1 mL) consisted of 1 mM ECOB (100 mM stock in DMSO), 0.2 mM NAD(P)H, 50 mM potassium phosphate (pH 6.5) buffer, and 5–10 μL of cell-free extract or 15 μg (for NADPH) or 30 μg (for NADH) of the purified reductase. One unit of reductase was defined as the quantity of enzyme required to catalyze the oxidation of 1 μmol NAD(P)H in 1 min at 30 °C.

The oxidation reaction mixture (1 mL) of formate dehydrogenase consisted of 10 mM sodium formate, 0.2 mM NAD$^+$, 50 mM potassium phosphate (pH 6.5) buffer, and 10 μL of commercial formate dehydrogenase. The reaction rate was monitored using a spectrophotometer based on the increase in absorbance at 340 nm for 5–10 min at 30 °C. One unit of formate dehydrogenase was defined as the quantity required to reduce 1 μmol of NAD$^+$ in 1 min at 30 °C.

2.3. Site-directed mutagenesis

Arg27, Ser259, Lys261, Arg264 and Ser260 residues were mutated into other selected amino acids using a QuikChange lightning site-directed mutagenesis kit (Stratagene). The PCR primers employed for the preparation of the mutants are provided in Supplementary data 1.

For the preparation of single mutants, the *S. cerevisiae* YDL124W gene (pETR124) was used as template DNA for the PCR reactions [19]. The reaction conditions were as follows: 30 cycles of denaturation at 95 °C for 20 s, annealing at 60 °C for 10 s, and polymerization at 72 °C for 3.5 min. After the PCR reaction, the reaction mixtures were treated with *Dpn*I at 37 °C for 5 min and subsequently transformed into *E. coli* XL10-Glod ultracompetent cells from QuikChange lightning site-directed mutagenesis kit. The recombinant plasmids were purified from the recombinant *E. coli* cells and their nucleotide sequences were analyzed to confirm the mutations.

For the preparation of double mutant enzymes, the R264H reductase gene was employed as template DNA for the PCR reactions. The PCR reaction conditions and the cloning methods were exactly the same as those used in the previous single mutant preparation.

2.4. Expression and purification of mutant reductases

The recombinant plasmids were transformed into *E. coli* BL21 (DE3) cells. *E. coli* cells containing each plasmid were cultured at 20 °C in Luria–Bertani medium (1% tryptone, 0.5% yeast extract and 0.5% NaCl) containing 100 μg/mL of ampicillin. When the cells reached an optical density ($OD_{600\,nm}$) of 0.5, expression was induced via the addition of 1 mM isopropyl thio-β-D-galactoside (IPTG). Cultivation was continued for an additional 24 h, after which the cells were harvested via 10 min of centrifugation at 10,000 × *g* at 4 °C and re-suspended in a 1/20 volume of 50 mM potassium phosphate buffer (pH 7.0).

The recombinant *E. coli* cells were disrupted by sonication and each mutant enzyme in the cell extracts was purified as follows. First, each cell-free extract was loaded onto Ni-NTA spin columns (QIAGEN GmbH, Hilden, Germany) equilibrated with a 50 mM potassium phosphate buffer (pH 7.0) containing 10 mM imidazole and 300 mM NaCl, then washed with the 50 mM imidazole buffer. The mutant reductases were then eluted from the column via the application of a 300 mM imidazole buffer. The active fractions were then collected and desalted using PD-MiniTrap G10 desalting columns (GE Healthcare Bio-Sciences AB, UK). The purified enzymes were analyzed by SDS-PAGE (Supplementary data 2) and their protein amounts were assayed through the Bradford method.

The secondary structures of wild-type and mutant, R264H and R264H/R27Y, were assessed by circular dichroism spectroscopy. The ellipticity was measured in the range 190–260 nm with a scanning speed of 100 nm/min in 1 s response time at 20 °C on a JASCO J-815 spectrometer. Spectra were obtained by the average of three successive spectra with purified enzyme at 50 mM potassium phosphate buffer (pH 7.0).

2.5. Kinetic studies of the mutant enzymes

Using the purified wild-type and six mutants (S260D, R264H, R264Y, R264H/R27Y, R264H/S259E, and R264H/S260E), kinetic studies were conducted. In order to elucidate the K_m and k_{cat} values of wild-type and mutants toward ECOB, enzyme assays were conducted in the reaction mixtures containing 1–15 mM ECOB, 0.5 mM NAD(P)H, and 0.19–14 μM purified enzyme. The K_m and k_{cat} values of each enzyme toward ECOB were calculated from the Lineweaver–Burk plots. Then, in order to determine the K_m values of the wild-type and mutants toward NAD(P)H cofactor, enzyme assays were conducted in the reaction mixtures containing excess ECOB (10-fold concentration of $K_{m\,ECOB}$) and 0.01–0.5 mM NAD(P)H cofactor, and 0.19–14 μM purified enzyme. The K_m values of each enzyme were calculated from the Lineweaver–Burk plots.

2.6. Molecular modeling

Molecular modeling was carried out using the SYBYL modeling package 8.1 (Tripos, Inc.). The previously reported homology model of the enzyme containing the substrate and NADPH was employed [19]. The AMBER99 force field [21] was used to describe the atom types of the enzyme containing the substrate and cofactor. Some missing parameters were adapted from the general AMBER force field (GAFF) [22]. Nonstandard partial charges were calculated using the Pullman method for the enzyme and the Gasteiger-Huckel method for the substrate and cofactor. A nonbonded cutoff distance of 8 Å and a distance-dependent dielectric function were employed in all calculations. Energy minimizations were conducted

with the Powell minimizer and continued until the rms derivatives fell below 0.005 kcal mol^{-1} Å^{-1}.

2.7. Enzymatic coupling reaction and reaction mixture analysis

The enantioselectivity of the enzymatic reduction of ECOB was evaluated. The general procedure was as follows: 10 mM ECOB, 1 mM NADH, 4.8 mg of purified reductase, 20 mM sodium formate, and 1.5 units of commercial formate dehydrogenase (toward NAD$^+$) were mixed in a total volume of 10 mL of potassium phosphate buffer (50 mM, pH 6.5), and the mixture was incubated at 25 °C.

ECHB product was extracted by ethyl acetate and dried via evaporation. After acetylation step and washing steps, the organic phase was subsequently analyzed using a GC system equipped with a Chirasil-dex column (Varian, Ltd) [19]. The column temperature was increased from 70 °C to 180 °C at a rate of 5 °C/min, and maintained for 2 min at 180 °C. By comparing the retention times and peak areas of standard (*R*)- and (*S*)-alcohol peaks, the total quantities of products in the reaction mixtures were calculated. The retention times of (*R*)- and (*S*)-alcohols were 16.8 min and 17.0 min, respectively.

3. Results and discussion

3.1. Construction of mutant reductases based on rational design

In a previous study, yeast YDL124W reductase was reported to convert ECOB substrate exclusively into the (*S*)-ECHB product [19]. In that conversion, YDL124W utilized NADPH as a cofactor, but not NADH. In that enzyme reaction, GDH was employed as a coupling enzyme for NADPH recycling (Scheme 1A). NADPH is, however, far more expensive and unstable than NADH. For this reason, the development of YDL124W mutant enzyme able to use NADH would render the production of (*S*)-ECHB more economical. In this new process, FDH can be employed for NADH recycling (Scheme 1B). This FDH coupling reaction provides an extra advantage; GDH produces gluconic acid and it may be cumbersome to adjust the reaction pH frequently in the middle of the reaction process, whereas FDH produces CO_2, and it is not essential that the reaction pH be adjusted during the reaction [1,3].

Homology model of YDL124W and its docking model with ECOB and NADPH were recently constructed [19]. In this research,

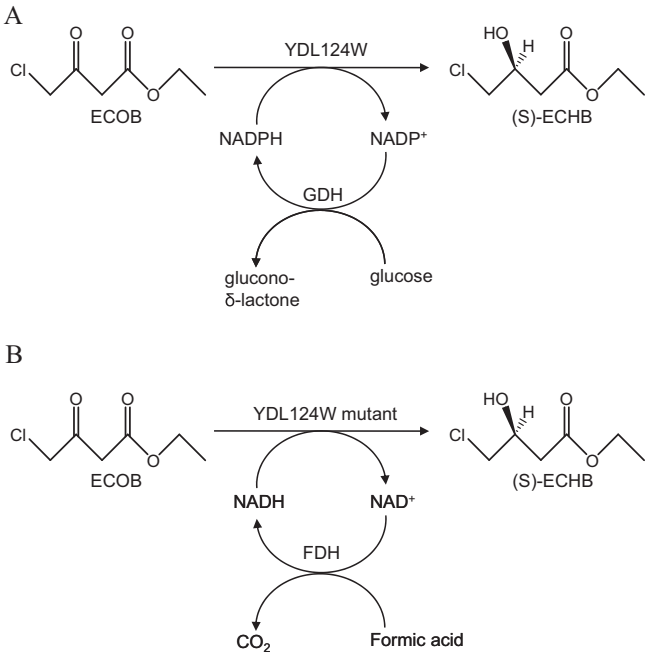

Scheme 1. Schematic presentation of two coupling reactions. (A) YDL124W reduces ECOB using the NADPH cofactor regenerated by glucose dehydrogenase (GDH). (B) YDL124W mutant reduces ECOB using the NADH cofactor regenerated by formate dehydrogenase (FDH).

structural analysis of the cofactor-binding site using the docking model suggested that the 2′-phosphate group of adenosine ribose of NADPH was surrounded by five amino acid residues including Arg27, Ser259, Ser260, Lys261, and Arg264. The two guanidino nitrogen atoms of Arg27 and Arg264 were located at a distance of 2.7–2.8 Å from the phosphate oxygen atoms, and seemed to form two salt bridges (Fig. 1). The hydroxyl groups of Ser259 and the ε-amino group of Lys261 were also located close and formed hydrogen bonds with the phosphate group; thus they made a hydrophilic pocket for the binding of the phosphate group of the adenosine ribose of NADPH. The S^{259}–S^{260}–K^{261}–x–x–R^{264} sequence was similar to the previously reported consensus sequence (K–S–x–x–x–x–R) [16]. Therefore, we

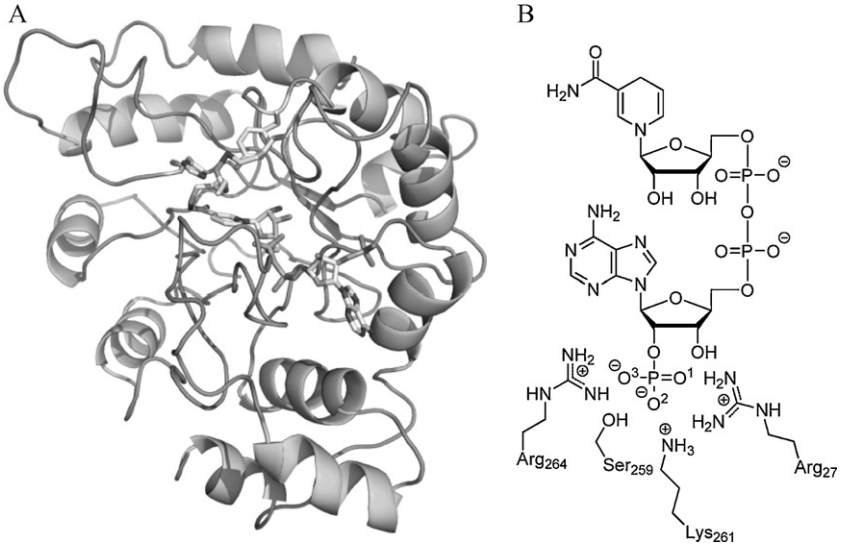

Fig. 1. Homology model of YDL124W and NADPH binding site. (A) The 3-dimensional homology model was redrawn on the basis of the previously reported structure [19]. (B) Line diagrams of a docking structure of YDL124W with NADPH. The phosphate group at 2′-O of the adenosine group is surrounded by Arg27, Ser259, Lys261, and Arg264.

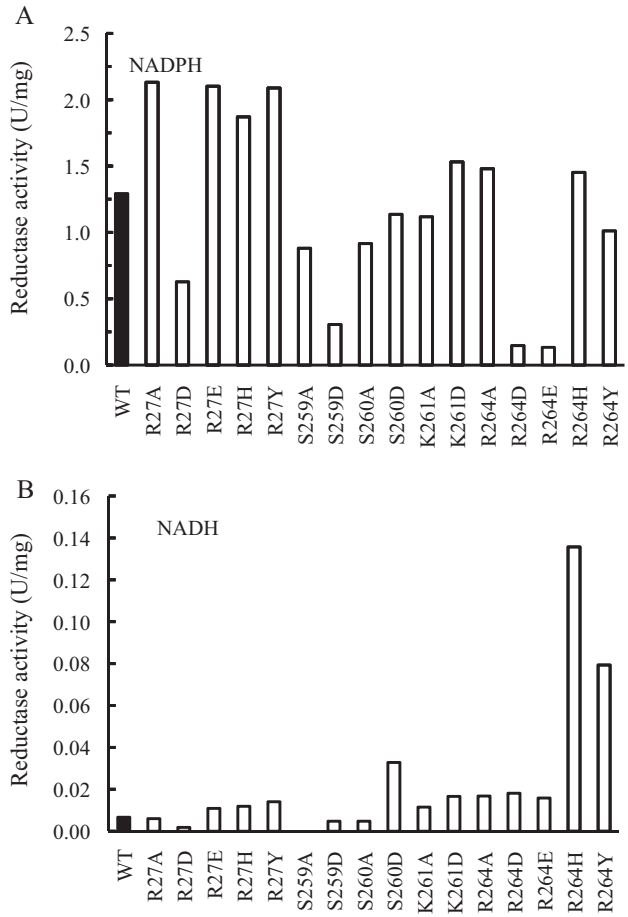

Fig. 2. Reductase activity of various single mutants. (A) Reductase activities were measured using NADPH cofactor. (B) Reductase activities were measured using NADH cofactor.

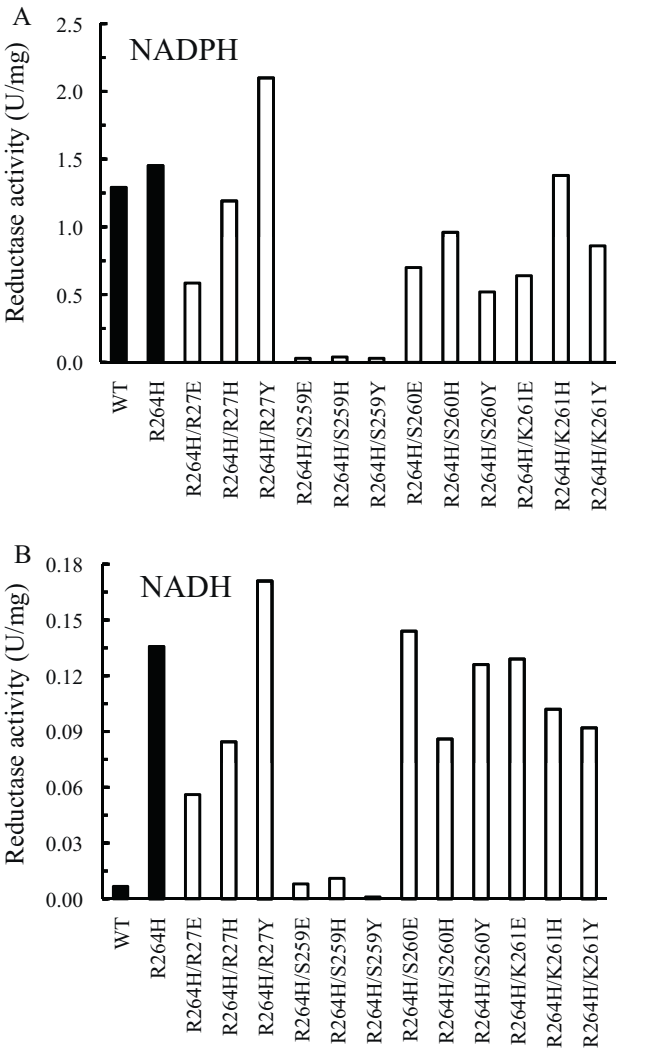

Fig. 3. Reductase activity of various double mutants. (A) Reductase activities were measured using NADPH cofactor. (B) Reductase activities were measured using NADH cofactor.

attempted to change this region, along with an additional residue (Arg27).

In this study, a variety of YDL124W mutants were constructed to make 'NADH-utilizing reductase'. At first, a total of 16 different single mutant enzymes were constructed; Arg27 and Arg264 were mutated into Ala, Asp, Glu, His, and Tyr, respectively. Additionally, Ser259, Ser260, and Lys261 were mutated into Ala and Asp, respectively. After the purification steps, the purities of mutant reductases were ascertained via SDS-PAGE (Supplementary data 2). When the purified mutant enzymes were tested for their reductase activities using ECOB and NADH as the substrate and cofactor, respectively, the majority of the mutants evidenced very little activity relative to the wild-type (Fig. 2). However, among them, two mutant enzymes (R264H and R264Y) evidenced profoundly increased reductase activities with the NADH cofactor. The purified R264H and R264Y exhibited specific activities of 0.136 and 0.079 U/mg, respectively, whereas the purified wild-type reductase exhibited a specific activity of 0.007 U/mg. Their reductase activities were increased by 19-fold and 11-fold, respectively.

Secondly, various double mutant enzymes were designed using R264H as a template enzyme. Arg27, Ser259, Ser260, and Lys261 were mutated into Glu, His, and Tyr, respectively. When the purified double mutant enzymes were assessed for reductase activity using the same method as the single mutant enzymes, they evidenced substantially different activities (Fig. 3). Among them, the R264H/R27Y mutant showed the most profoundly enhanced activities in comparison with R264H. The purified R264H/R27Y exhibited a specific activity of 0.171 U/mg, which was 24-fold higher than that of the wild-type.

3.2. Kinetic parameters of mutant reductases

In order to elucidate the enzyme activities in the presence of NADPH or NADH cofactor, kinetic studies were conducted against six mutants, as well as wild-type reductase (Table 1). The six mutants tested included S260D, R264H, R264Y, R264H/R27Y, R264H/S259E, and R264H/S260E. As anticipated, the wild-type enzyme not only had a very low K_m value (0.00436 mM) for NADPH but also a very high K_m value (43.6 mM) for NADH. Moreover, the $k_{cat}/K_{m\ ECOB}$ ($104\ min^{-1}\ mM^{-1}$) in the presence of NADPH cofactor was quite a bit higher than that ($0.453\ min^{-1}\ mM^{-1}$) seen in the presence of the NADH cofactor.

Most mutants evidenced rather elevated K_m values (0.03–0.9 mM) toward NADPH compared to the wild-type (0.00436 mM). Conversely, many of the mutants had substantially reduced K_m values (0.05–4 mM) toward NADH relative to the wild-type (43.6 mM). In the case of R264H, the K_m value for NADH was 1.15 mM, which suggested that the NADH cofactor was bound tightly within the active pocket of the mutant enzyme. R264H/R27Y evidenced the lowest K_m value of 0.058 mM. These two mutants exhibited substantially elevated $k_{cat}/K_{m\ ECOB}$ values with the NADH

Table 1
Kinetic parameters of wild-type and mutant reductase enzymes.

	NADPH				NADH			
	$K_{m\ cofactor}$ (mM)	$K_{m\ ECOB}$ (mM)	k_{cat} (min^{-1})	$k_{cat}/K_{m\ ECOB}$ ($min^{-1}\ mM^{-1}$)	$K_{m\ cofactor}$ (mM)	$K_{m\ ECOB}$ (mM)	k_{cat} (min^{-1})	$k_{cat}/K_{m\ ECOB}$ ($min^{-1}\ mM^{-1}$)
WT	0.00436	1.08	112	104	43.6	10.2	4.62	0.453
S260D	0.0350	1.21	171	141	4.18	3.39	14.8	4.37
R264H	0.0660	7.69	507	65.9	1.15	1.73	63.9	36.9
R264Y	0.0390	3.77	288	76.4	0.354	4.49	31.9	7.10
R264H/R27Y	0.0740	8.10	759	93.7	0.0580	1.15	34.1	29.7
R264H/S259E	0.991	3.83	1.90	0.496	ND	31.6	1.21	0.0383
R264H/S260E	0.143	26.3	1240	47.1	0.374	2.35	35.9	15.3

ND, not detected.

cofactor (36.9 and 29.7 $min^{-1}\ mM^{-1}$, respectively) compared to that of the wild-type with NADH cofactor (0.453 $min^{-1}\ mM^{-1}$); these values were 82- and 66-fold higher than those of the wild-type (Table 1). Circular dichroism results indicated that the secondary structures of both R264H and R264H/R27Y were almost the same as that of the wild-type (Supplementary data 3).

Although the $k_{cat}/K_{m\ ECOB}$ values of R264H and R264H/R27Y mutants with NADH were slightly lower than that (104 $min^{-1}\ mM^{-1}$) of wild-type with NADPH, they seemed to have sufficiently high activities for the production of (*S*)-ECHB using NADH cofactor.

3.3. Molecular basis of utilizing NADH as a cofactor by the mutants

In order to analyze the binding affinity of NADPH or NADH to the wild-type or R264H mutant enzyme, we generated three other docking structures from the docking model of the wild-type enzyme containing the ECOB and NADPH via the substitution of NADPH with NADH or replacement of the Arg264 residue with His. After substitution, we minimized all four models of the docking structures and analyzed the phosphate-binding region (Table 2).

An energy-minimized structure of the wild-type enzyme with NADPH demonstrated that the negatively charged phosphate group at the adenosine group is stabilized by several positively charged amino acids, such as two Arg and one Lys (Fig. 4A). Additionally, a Ser residue made hydrogen bonds with an oxygen atom of the phosphate group. The distances between the oxygen atoms of the phosphate group and the terminal nitrogen of Arg or Lys were measured at 2.5–2.8 Å. The oxygen atoms (Oγ) of the Ser and the phosphate are separated by a distance of 2.5–3.0 Å. The distances represent typical hydrogen bonding in a protein. These electronic interaction and hydrogen bonds are presumably a key interaction for the acceptance of NADPH as a cofactor.

On the other hand, hydrogen bonds were not found in the docking structure of the wild-type enzyme with NADH (Fig. 4B). NADH does not have a negatively charged phosphate group; thus no electronic interaction is possible. The positively charged residues repelled one another and moved away from the ribose ring of the adenosine group. Therefore, the YDL124W enzyme would not efficiently utilize NADH as a cofactor.

A minimized model of the R264H mutant enzyme with NADPH demonstrated that all hydrogen bonds from Arg27, Ser259, and Lys261 to the phosphate group are available (Fig. 4C). Additionally, the protonated nitrogen atom (Nδ) [23] of the His serves a hydrogen bond donor similar to the Arg, although the His is incapable of neutralizing the negative charge of the phosphate group. Additionally, the imidazole ring of the His264 residue exhibited a stacking interaction with the adenosine base of NADPH. This presumably explains how the Arg264His mutant can still accept NADPH as a cofactor.

A docking model of the R264H mutant enzyme with NADH also evidenced a similar hydrogen bonding interaction with the residues, except for the Lys261 residue (Fig. 4D). The 2′-oxygen

Table 2
Hydrogen bonds in possible docking structures of the wild type and Arg264His mutant enzyme with NADPH or NADH.

	Atom of residue	Atom of cofactor	Distance[a]
NADPH			
Wild type	Nω (Arg27)	O1 of the phosphate P2′	2.8 Å
	Oγ (Ser259)	O2 and O3 of the phosphate P2′	2.5 and 3.0 Å
	Nζ (Lys261)	O1 and O2 of the phosphate P2′	2.5 and 2.6 Å
	Nω (Arg264)	O1 and O3 of the phosphate P2′	2.7 and 2.8 Å
NADH			
Wild type	Nω (Arg27)	O2′ of the adenosine ribose	4.0 Å
	Oγ (Ser259)	O2′ of the adenosine ribose	4.7 Å
	Nζ (Lys261)	O2′ of the adenosine ribose	7.0 Å
	Nω (Arg264)	O2′ of the adenosine ribose	4.8 Å
NADPH			
R264H mutant	Nω (Arg27)	O1 and O2 of the phosphate P2′	2.7 and 2.8 Å
	Oγ (Ser259)	O2 of the phosphate P2′	2.4 Å
	Nζ (Lys261)	O1 and O2 of the phosphate P2′	2.7 and 2.7 Å
	Nδ (His264)	O3 of the phosphate P2′and O2′ of the adenosine ribose	2.9 and 3.0 Å
NADH			
R264H mutant	Nω (Arg27)	O2′ of the adenosine ribose	3.1 Å
	Oγ (Ser259)	O2′ of the adenosine ribose	3.1 Å
	Nζ (Lys261)	O2′ of the adenosine ribose	7.0 Å
	Nδ (His264)	O2′ of the adenosine ribose	2.9 Å

[a] Distance between non-hydrogen atoms (N—O or O—O). Distances of 2.7–3.2 Å are considered as a range for a hydrogen bond.

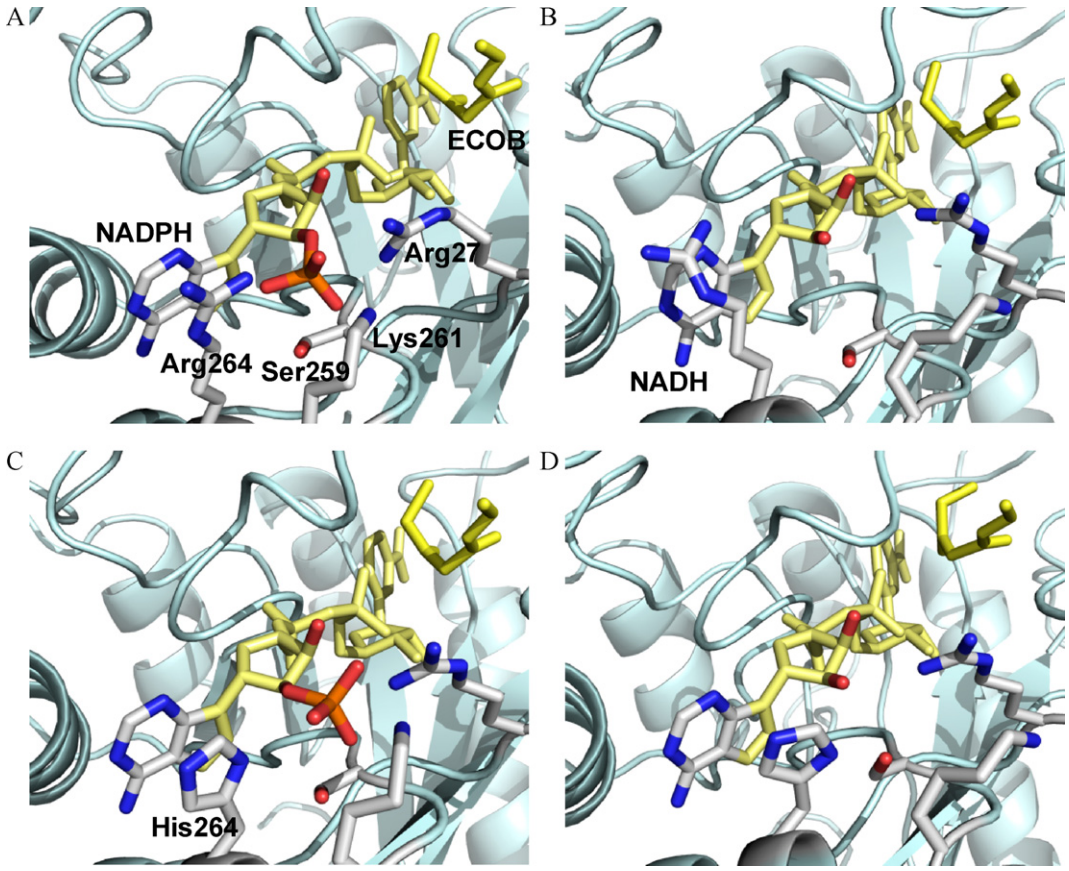

Fig. 4. Proposed ECOB and NADPH or NADH binding structures. (A) Wild-type enzyme with NADPH. (B) Wild-type enzyme with NADH. (C) Arg264His mutant enzyme with NADPH. (D) Arg264His mutant enzyme with NADH. ECOB (yellow), NADPH or NADH (yellow and atomic color), Arg27, Ser259, Lys261, Arg264, and His264 were represented as a stick model. The imidazole ring of the His264 evidenced a stacking interaction with the adenosine base of NADPH or NADH (distance: ~3.5–4.3 Å). (For interpretation of the references to color in figure caption, the reader is referred to the web version of the article.)

atom of the ribose ring is stabilized by hydrogen bonds with Ser259 and Arg27. The positive charges of the Arg27 and Lys261 residues repel each other, and only one of the residues could function as a hydrogen bond donor. Additionally, the unprotonated nitrogen atom (Nδ) of the His264 residue appears likely to produce hydrogen bonds to the 2′-oxygen atom of the terminal ribose ring of NADH and the imidazole ring of the histidine has a stacking interaction with the adenosine base. These interactions presumably explain the Arg264His mutant enzyme can accept NADH with the lower K_m value relative to the wild-type enzyme.

Additionally, we modeled the double mutant enzyme (R264H/R27Y) containing ECOB and NADH (Fig. 5). This mutant enzyme possesses a lower K_m value for NADH relative to the wild-type and the R264H mutant enzyme. The 2′-oxygen atom of the ribose ring can make hydrogen bonds to Ser259 (3.2 Å), Lys261 (3.0 Å), and His264 (3.0 Å). The Tyr27 residue exhibits no interaction with the 2′-oxygen atom. However, unlike the R264H mutant enzyme, the Lys261 residue, which is located away from the 2′-oxygen atom in a docking model of the R264H mutant enzyme with NADH (Fig. 4B), functions as a hydrogen bond donor. The substitution of Arg27 with tyrosine looses a hydrogen bond between the Arg27 residue and the 2′-oxygen atom, but gains hydrogen bonding between the 2′-oxygen atom and Lys261 because the repulsive interaction between Arg27 and Lys261 residues is diminished, and thus the Lys can be brought closer to the oxygen atom. Additionally, the Tyr27 residue possesses a weak hydrogen bond (3.4 Å) with the 3′-oxygen atom. These interactions may reduce the K_m value for NADH.

3.4. Mutant reductase and FDH coupling reaction

Bioconversions of the wild-type and two mutants (R264H and R264H/R27Y) were conducted using NADH and commercial FDH

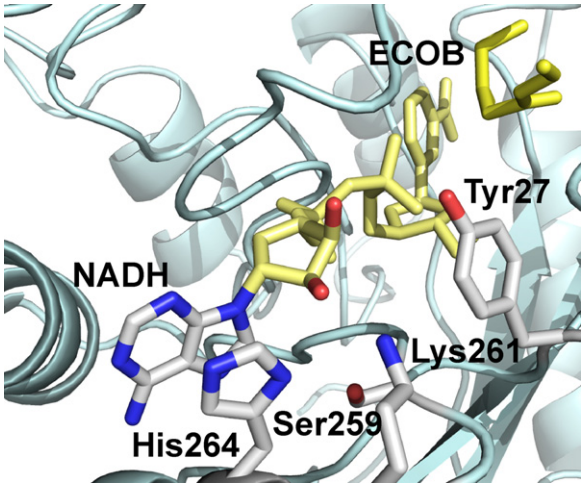

Fig. 5. A proposed ECOB and NADH binding structure of the R264H/R27Y mutant enzyme. The color and representation were identical to those in Fig. 4. The 2′-oxygen atom of the ribose ring hydrogen bonds to Ser259 (3.2 Å), Lys261 (3.0 Å), and His264 (3.0 Å). The Tyr27 residue evidences a weak interaction with the 3′-oxygen atom (3.4 Å). (For interpretation of the references to color in figure caption, the reader is referred to the web version of the article.)

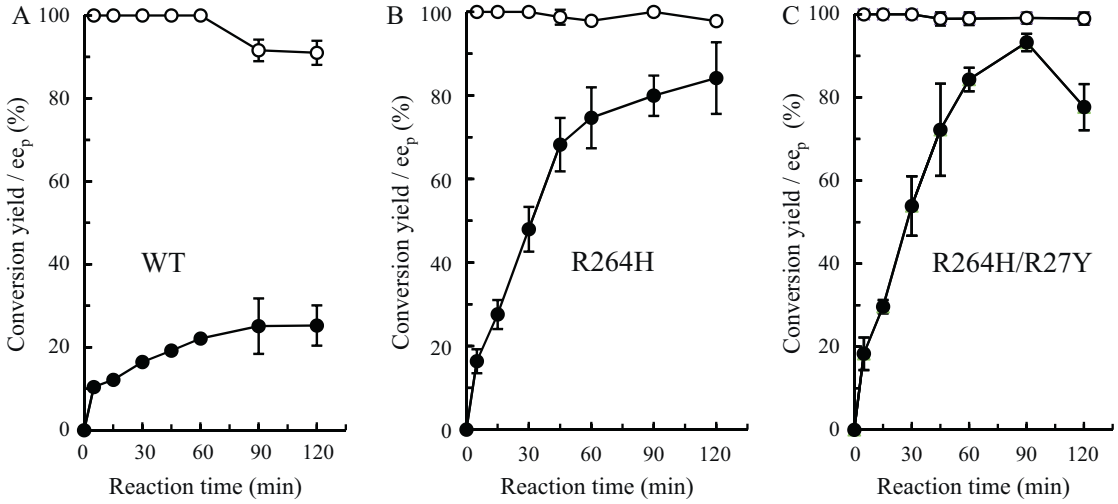

Fig. 6. Bioconversion using mutant reductases. Wild-type (A), R264H (B), and R264H/R27Y (C) were used in the bioconversion of ECOB into (*S*)-ECHB together with FDH and NADH. Closed and open circles represent the conversion yield and e.e.$_p$, respectively.

as a cofactor and coupling enzyme, respectively. In the case of wild-type (Fig. 6A), the bioconversion yield and rate were 25% and 2.66 μmol h^{-1} mg^{-1}, respectively. These low yield and slow conversion rates were anticipated as the wild-type had a very low k_{cat}/K_m value (0.453 min^{-1} mM^{-1}) with NADH cofactor (Table 1). Moreover, the wild-type showed an unexpected reduction in enantiomeric excess of 91% for (*S*)-ECHB when NADH was employed as a cofactor. This lower e.e. value seemed to be related with its high K_m value (10.2 mM) toward ECOB (Table 1).

However, in the case of R264H and R264H/R27Y, we noted a conversion yield of 84% and 93%, respectively, within 120 min of reaction (Fig. 6B and C). The conversion rates were 18.9 and 20.1 μmol h^{-1} mg^{-1}, respectively, which were approximately 7-fold higher than that of the wild-type. These results clearly demonstrated that the two mutants could utilize NADH as a cofactor, which was continuously recycled by FDH. The single mutant and the double mutant produced (*S*)-ECHB enantioselectively with e.e.$_p$ values of 98% and 99%, respectively.

4. Conclusion

We developed several YDL124W mutants capable of using NADH as a cofactor by rational design in this study. Among them, the R264H and R264H/R27Y mutants evidenced very low K_m values toward NADH and highly increased k_{cat}/K_m values toward ECOB. Although the k_{cat}/K_m values were still less than that of the wild-type toward NADPH, the two mutants could carry out the bioconversion efficiently in the presence of NADH and FDH as the cofactor and coupling enzyme, respectively. These results suggest that these mutants can be employed for the economic production of (*S*)-ECHB.

Acknowledgments

This work was supported by the 21C Frontier Microbial Genomics and Applications Center Program, Ministry of Education, Science & Technology, Republic of Korea, and by Basic Science Research Program through the National Research Foundation of Korea (NRF) funded by the Ministry of Education, Science and Technology (2011-0009692) and the 2011 Research Fund of the Catholic University of Korea. We appreciate the KRICT for utilizing the SYBYL package.

Appendix A. Supplementary data

Supplementary data associated with this article can be found, in the online version, at doi:10.1016/j.molcatb.2012.01.016.

References

[1] K. Goldberg, K. Schroer, S. Lűtz, A. Liese, Appl. Microbiol. Biotechnol. 76 (2007) 237–248.
[2] J.C. Moore, D.J. Pollard, B. Kosjek, P.N. Devine, Acc. Chem. Res. 40 (2007) 1412–1419.
[3] A. Weckbecker, H. Gröger, W. Hummel, Adv. Biochem. Eng. Biotechnol. 120 (2010) 195–242.
[4] Y.H. Choi, H.J. Choi, D. Kim, K.N. Uhm, H.K. Kim, Appl. Microbiol. Biotechnol. 87 (2010) 185–193.
[5] H.J. Park, J. Jung, H.J. Choi, K.N. Uhm, H.K. Kim, J. Microbiol. Biotechnol. 20 (2010) 1300–1306.
[6] Q. Ye, P. Ouyang, H. Ying, Appl. Microbiol. Biotechnol. 89 (2011) 513–522.
[7] M. Bozic, S. Pricelius, G.M. Guebitz, V. Kokol, Appl. Microbiol. Biotechnol. 85 (2010) 563–571.
[8] R. Kratzer, M. Pukl, S. Egger, M. Vogl, L. Brecker, B. Nidetzky, Biotechnol. Bioeng. 108 (2010) 797–803.
[9] K. Schroer, U. Mackfeld, I.A.W. Tan, C. Wandrey, F. Heuser, S. Bringer-Meyer, A. Weckbecker, W. Hummel, T. Daussmann, R. Pfaller, A. Liese, S. Lűtz, J. Biotechnol. 132 (2007) 438–444.
[10] V.Z. Pletnev, C.M. Weeks, W.L. Duax, Proteins 57 (2004) 294–301.
[11] S. Banta, B.A. Swanson, S. Wu, A. Jarnagin, S. Anderson, Protein Eng. 15 (2002) 131–140.
[12] M. Katzberg, N. Skorupa-Parachin, M.F. Gorwa-Grauslund, M. Bertau, Int. J. Mol. Sci. 11 (2010) 1735–1758.
[13] G.A. Khoury, H. Fazelinia, J.W. Chin, R.J. Pantazes, P.C. Cirino, C.D. Maranas, Protein Sci. 18 (2009) 2125–2138.
[14] S. Watanabe, A. Abu Saleh, S.P. Pack, N. Annaluru, T. Kodaki, K. Makino, Microbiology 153 (2007) 3044–3054.
[15] R. Zhang, Y. Xu, Y. Sun, W. Zhang, R. Xiao, Appl. Environ. Microbiol. 75 (2009) 2176–2183.
[16] S. Banta, S. Anderson, J. Mol. Evol. 55 (2002) 623–631.
[17] M. Wada, H. Kawabata, A. Yoshizumi, M. Kataoka, S. Nakamori, Y. Yasohara, N. Kizaki, J. Hasegawa, S. Shimizu, J. Biosci. Bioeng. 87 (1999) 144–148.
[18] N. Kizaki, Y. Yasohara, J. Hasegawa, M. Wada, M. Kataoka, S. Shimizu, Appl. Microbiol. Biotechnol. 55 (2001) 590–595.
[19] J. Jung, H.J. Park, K.N. Uhm, D. Kim, H.K. Kim, Biochim. Biophys. Acta 1804 (2010) 1841–1849.
[20] L. Di Costanzo, J.E. Drury, T.M. Penning, D.W. Christianson, J. Biol. Chem. 283 (2008) 16830–16839.
[21] J. Wang, P. Cieplak, P.A. Kollman, J. Comput. Chem. 21 (2000) 1049–1074.
[22] J. Wang, W. Wang, P.A. Kollman, D.A. Case, J. Mol. Graph. Model. 25 (2006) 247–260.
[23] J.L. Sudmeier, E.M. Bradshaw, K.E. Haddad, R.M. Day, C.J. Thalhauser, P.A. Bullock, W.W. Bachovchin, J. Am. Chem. Soc. 125 (2003) 8430–8431.